Journal of Sound and Vibration (2003) **259**(3), 571–583
doi:10.1006/jsvi.2002.5095, available online at http://www.idealibrary.com on IDEAL®

THE SWING VIBRATION, TRANSVERSE OSCILLATION OF CRACKED ROTOR AND THE INTERMITTENCE CHAOS

W. Y. Qin,† G. Meng and T. Zhang

State Key Lab of Vibration, Shock and Noise, Shanghai Jiao Tong University, 1954 *Hua Shan Road, Shanghai* 200030, *People's Republic of China*

(*Received* 4 *May* 2001, *and in final form* 2 *April* 2002)

This paper studies the non-linear dynamic response of a cracked rotor by taking the swing vibration of disc into consideration. The results show that if a small crack appears, the frequency of transverse oscillation is synchronous with rotating speed ratio (Ω), and the frequency of swing vibration is $N\Omega(N=1,2,\ldots)$. As the crack increases, the response becomes chaotic in some range of Ω. The deeper the crack is, the wider the chaotic range of Ω is. Routes to chaos include intermittence to chaos and quasi-period to chaos. When the crack is fairly deep, some new resonance regions develop. In these regions, the response becomes infinity rapidly. The appearance of intermittence chaos is induced by the frequent frustration of stable oscillation, which is resulted from the continuous increase of swing amplitude. Unbalance parameter U is effective in suppressing chaos. Crack angle β cannot affect the essence of response, but can influence the amplitude of synchronous response.

1. INTRODUCTION

Fatigue cracking of a rotor shaft may cause catastrophic damage to rotating machinery, as reported by Jack and Patterons [1]. So, detailed investigation into the dynamic response of a rotor with crack in the shaft is very important for diagnosing and preventing rotor cracks.

Cracked rotor is a time variable, highly non-linear system. Recently, many papers have been published on the non-linear response and stability of rotor with opening and closing crack.

Muller [2] applied theory of Lyapunov exponents to non-smooth dynamical system with a cracked rotor, and found the chaotic motion and strange attractor. Sekhar [3] studied the dynamic response of a rotor containing two open cracks by finite element method, the influence of one crack over another with regard to eigenfrequencies, mode shapes and threshold speed limits was observed. Zheng [4] pointed out that fatigue crack is an important reason for the existence of lower frequency vibration components in turbo-machines and a small fatigue crack may drive a system into instability in a very short time. Lees [5] studied an asymmetric beam mounted horizontally and having a transverse crack, the results had shown that as the orientation of the rotor is varied, a complicated pattern of responses appears due to the opening and closing of the crack. The complex behavior arises because of the rotation of the beam's principal axes. Meng [6] investigated the stability and the stability degree of a cracked flexible rotor supported on different kinds of

†Now at Northwestern Polytechnical University, Xian 710072, P.R.C.

0022-460X/02/$35.00

journal bearings and gave the unstable zone caused by rotor crack, the gravity parameter has evident influence on the system's stability and stability degree. Zheng [7] studied the bifurcation and chaos of cracked rotor and found that when stiffness change ratio ΔK is large, the quasi-periodic and chaotic responses appear near $1/2\Omega$, $2/3\Omega$, and there are two kinds of bifurcation from period to quasi-period.

But most of the models omitted the presence of swing vibration of discs. For a rotor system, the swing vibration means that the inclination angle of shaft at the disc's position is variable with time. As shown in Figure 1, for Jeffcott rotor, since the disc is mounted at mid-span of the shaft, there is no gyroscopic moment on the disc if there is no crack. Under this condition, there is no swing vibration of the disc. But when crack appears near the disc, the moment of inertia of the shaft section at the crack position becomes smaller. This leads to the asymmetry of stiffness of shaft at the left and right side of the disc. This asymmetry causes the disc to swing under the effect of gyroscopic moment, so that the inclination angle of the disc varies with time. The transverse oscillation and swing vibration constitutes the movement of the rotor system.

This paper investigates the non-linear response of cracked rotor by considering the opening and closing behavior of the crack, with emphasis on chaos, routes to chaos and relation between swing vibration and transverse oscillation. The ratio of moment of inertia of cross-section (p) is introduced to describe the degree of crack instead of ΔK (ratio of stiffness change). ΔK_l (change of transverse stiffness) and ΔK_θ (change of angular stiffness) can be expressed as a function of p.

2. EQUATION OF MOTION OF THE CRACKED ROTOR

A flexible Jeffcott rotor model is considered consisting of a rigid disc and a shaft with crack supported by two rigid bearings, as shown in Figure 1, using fixed co-ordinate

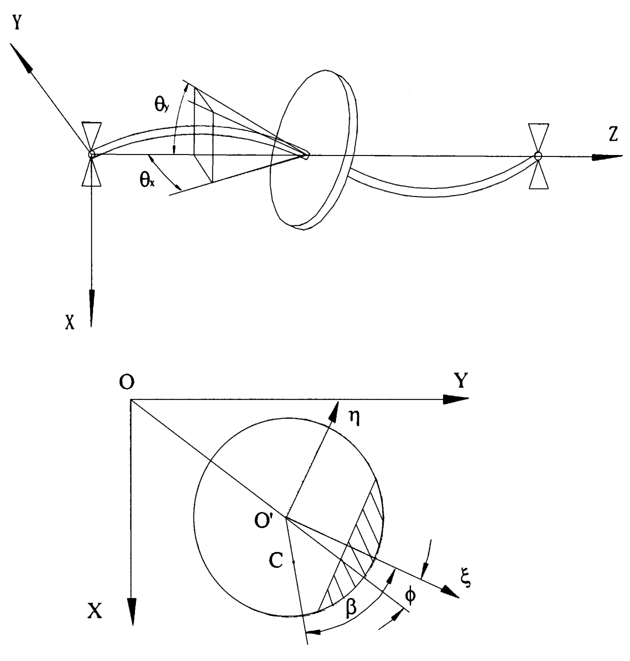

Figure 1. Schematic diagram of a cracked rotor.

system ($OXYZ$) and a rotating co-ordinate system ($O'\xi\ \eta Z$). The crack is at mid-span of the shaft and at the left side of the disc. The swing vibration is the variation of inclination angle of the shaft at the disc's position.

Although the actual crack on the shaft opens and closes gradually while rotating, the typical "on–off" model still can reflect the characteristic of crack and is applied in most cases. We use the step function to represent the opening and closing of the crack.

The equations of motion of the system can be written as

$$\begin{aligned} &m\ddot{x} + c_d\dot{x} + (k - f\cdot \Delta k\cos^2\omega t)x - (f\cdot\Delta k\sin\omega t\cos\omega t)y + f\cdot k_{12}\theta_y \\ &\qquad = me\omega^2\cos(\omega t+\beta+\phi_e) + mg, \\ &m\ddot{y} + c_d\dot{y} + (k - f\cdot \Delta k\sin^2\omega t)y - (f\cdot\Delta k\sin\omega t\cos\omega t)x - f\cdot k_{12}\theta_x \\ &\qquad = me\omega^2\sin(\omega t+\beta+\phi_e), \end{aligned} \tag{1.1}$$

$$\begin{aligned} &J_d\ddot{\theta}_y - J_p\omega\dot{\theta}_x + (k_\theta - f\cdot\Delta k_\theta\sin^2\omega t)\theta_y + (f\cdot\Delta k_\theta\sin\omega t\cos\omega t)\theta_x + f\cdot k_{12}x = 0 \\ &J_d\ddot{\theta}_x + J_p\omega\dot{\theta}_y + (k_\theta - f\cdot\Delta k_\theta\cos^2\omega t)\theta_x + (f\cdot\Delta k_\theta\sin\omega t\cos\omega t)\theta_y - f\cdot k_{12}y = 0, \end{aligned} \tag{1.2}$$

where m is the mass of the disc, k is the bending stiffness of the uncracked rotor, and k_θ is the angular stiffness. k_ξ and $k_{\theta\xi}$ are the bending stiffness in ξ direction and the angular stiffness, respectively, when the crack is open. k_{12} is the cross stiffness of the shaft in transverse and inclination direction. ϕ_e is the original phase angle. f is a switch function, whose value is variable with ϕ and can be written as

$$f(\phi) = \begin{cases} 1, & \phi = 0 \sim \pi/2,\ \ 3\pi/2 \sim 2\pi, \\ 0, & \phi = \pi/2 \sim 3\pi/2. \end{cases} \tag{2}$$

Δk and Δk_θ are the stiffness changing of the rotor with periodic opening and closing of the crack and can be represented as follows:

$$\begin{aligned} \Delta k &= k - k_\xi, \\ \Delta k_\theta &= k_\theta - k_{\theta\xi}, \end{aligned} \tag{3}$$

But Δk and Δk_θ are not independent of each other. Bending and angular stiffness of the shaft are both derived from system parameters on the basis of material mechanics. So considering boundary conditions, solving the elastic equation of beam with circular cross-section, we can get the following expressions:

$$k_\xi = s(1+p), \quad k_{\theta\xi} = sl^2(1+p), \quad k_{12} = -sl(1-p), \tag{4}$$

where s is a coefficient ($s = 3EI_0/l^3$), $p = I_z/I_0$, I_z is the moment of inertia of cross-section at crack position, whereas I_0 is at uncracked position.

Supposing δ is static deflection of the disc, dividing both sides of equation (1.1) by $\mathrm{m}\delta\omega^2$ and equation (1.2) by $J_d\omega^2$, the non-dimensional form of equation (1) can be obtained:

$$\begin{aligned} &X'' + \frac{2D}{\Omega}X' + \left(\frac{1}{\Omega^2} - \frac{f\cdot\Delta k_d}{\Omega^2}\cos^2\tau\right)X - \frac{f\cdot\Delta k_d}{\Omega^2}\sin\tau\cos\tau\, Y + \frac{f\cdot k_1}{\Omega^2}\theta_y = \frac{1}{\Omega^2} + U\cos(\tau+\beta+\phi_e), \\ &Y'' + \frac{2D}{\Omega}Y' + \left(\frac{1}{\Omega^2} - \frac{f\cdot\Delta k_d}{\Omega^2}\sin^2\tau\right)Y - \frac{f\cdot\Delta k_d}{\Omega^2}\sin\tau\cos\tau X - \frac{f\cdot k_1}{\Omega^2}\theta_x = U\sin(\tau+\beta+\phi_e), \\ &\theta_y'' - 2\theta_x' + \left(\frac{1}{\Omega^2} - \frac{f\cdot\Delta k_a}{\Omega_1^2}\sin^2\tau\right)\theta_y + \frac{f\cdot\Delta k_a}{\Omega_1^2}\sin\tau\cos\tau\theta_x + \frac{f\cdot k_2}{\Omega_1^2}X = 0, \\ &\theta_x'' + 2\theta_y' + \left(\frac{1}{\Omega^2} - \frac{f\cdot\Delta k_a}{\Omega_1^2}\cos^2\tau\right)\theta_x + \frac{f\cdot\Delta k_a}{\Omega_1^2}\sin\tau\cos\tau\theta_y - \frac{f\cdot k_2}{\Omega_1^2}Y = 0, \end{aligned} \tag{5}$$

where D is the external damping ratio and

$$(\,'\,) = \frac{\mathrm{d}}{\mathrm{d}\tau}, \qquad \tau = \omega t, \qquad k_1 = \frac{k_{12}}{\delta}, \qquad k_2 = \frac{k_{12}\delta}{k_\theta},$$

$$\Delta k_d = \frac{\Delta k}{k}, \qquad \Delta k_a = \frac{\Delta k_\theta}{k_\theta}, \qquad \Omega = \frac{\omega}{\sqrt{k/m}}, \qquad \Omega_1 = \frac{\omega}{\sqrt{k_\theta/J_d}}. \tag{6}$$

3. NON-LINEAR RESPONSE OF SYSTEM

Equation (5) is solved by the Simulink toolbox in Matlab, the switch function f is simulated with a switch box. The differential equations are solved by the fifth order Runge–Kutta method with variable time step.

From the numerical simulation results, it is found that the response before the first 500 T is generally not real due to the influence of free decreasing vibration, the exact period value depends on the external damping. So the following results are all obtained after the first 800 T (here T is the period of simulating force, it is equal to the time of a revolution of the rotor).

The methods used to analyze non-linear vibration are Poincarè diagram, bifurcation diagram, power spectrum and diagram of wave form. But for intermittence chaos, the above methods are not very effective in showing the characteristic and grade of intermittence. So in this paper, a new analysis method, which is called diagram of time phase, is proposed. The diagram of time phase is the point sets that are sampled at interval of T; so it can be regarded as a kind of diagram of time series. The diagram of time phase is not a Poincaré map, but it comes from a Poincaré map. Generally to construct a Poincaré map, X and X' are sampled at an interval of $T(\omega T = 2\pi)$, respectively, and then form point sets on X–X' plane. So the diagram of time phase shows the periodic characteristic of response. In this diagram, simple periodic response corresponds to a straight line (constituted with discrete points), quasi-periodic response corresponds to an orderly periodic curve (constituted with discrete points) and chaos corresponds to out-of-order points. It should be stressed here that the diagram of time phase is used only to describe the characteristics of intermittence chaos, for periodic and quasi-periodic the Poincaré and bifurcation diagrams are better.

With the change of rotating speed ratio Ω, the ratio of moment of inertia of cross-section p (corresponding to depth of crack), the crack angle β and the unbalance U, the system responses are calculated, respectively, and the following results can be deduced.

3.1. RELATION BETWEEN TRANSVERSE OSCILLATION AND SWING VIBRATION

The swing vibration is very sensitive to the occurrence of crack in the shaft. If there is no crack, there is no swing vibration, and the transverse oscillation is synchronous with rotating speed. If a small crack appears, the disc oscillates at a frequency of Ω (rotating speed ratio), and the swing vibration is composed of harmonic components ($N\Omega$, $N = 1, 2, \ldots$).As shown in Figure 2 (X_{AM} and θ_{AM} are the value of power spectrum density of transverse oscillation and swing vibration amplitude, respectively), when $\Omega = 0{\cdot}3$, for a small crack ($p = 0{\cdot}98$), the transverse oscillation is the main harmonic response, but the $1X$, $2X$, $3X$, $5X$ harmonic components can be seen in the diagram of power spectrum of swing vibration. For very small crack, oscillation is insensitive to the occurrence of crack, there is no evident change in the amplitude of vibration. So swing vibration can be used to determine the occurrence of small crack fault, especially for a crack in the early stage. But

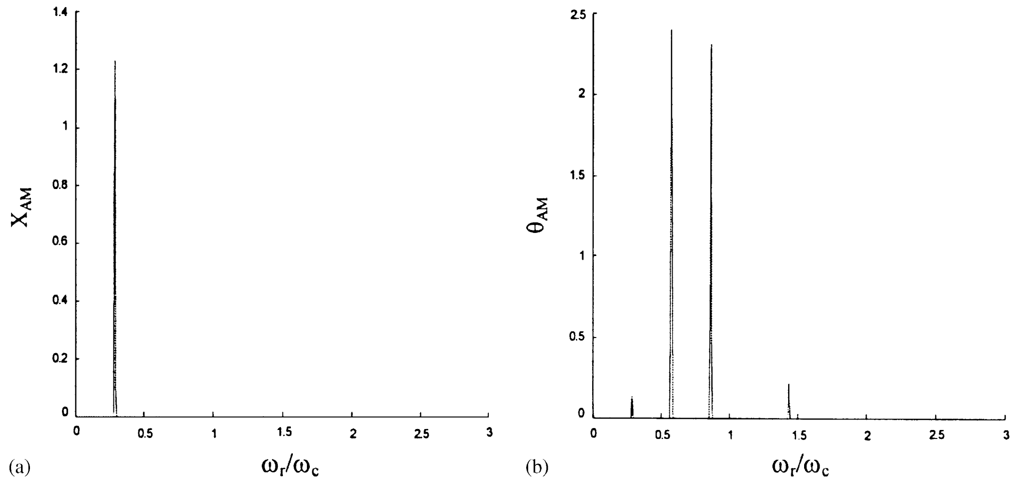

Figure 2. Comparison of power spectrums of transverse oscillation and swing vibration ($p=0{\cdot}98$, $D=0{\cdot}01$, $\Omega=0{\cdot}3$): (a) transverse oscillation and (b) swing vibration.

the essence of swing vibration is the same as transverse oscillation, if oscillation is periodic, quasi-periodic or chaotic, swing vibration has the same kind movement.

3.2. INFLUENCES OF SPEED RATIO(Ω) AND INERTIA MOMENT RATIO OF SHAFT SECTION (P)

When the crack is small ($p>0{\cdot}85$), the transverse oscillation is synchronous with Ω, whereas the swing vibration includes many harmonic components. If the crack is fairly large ($0{\cdot}4<p<0{\cdot}85$), in some range of Ω, chaos will happen. The routes to chaos are mainly intermittence to chaos and quasi-periodic to chaos. Figure 3 shows the process of entering and exiting chaos with the change of Ω. When $\Omega=1{\cdot}3536$, the response is period 1 (Figure 3(a)). As Ω increases, doubling periodic bifurcation happens, the response becomes period 2 (Figure 3(b)). Then the second-Hopf bifurcation happens and the response becomes quasi-periodic (Figure 3(c)). When $\Omega=1{\cdot}3646$, the response becomes chaos (Figure 3(d)). With the further increase of Ω, the response exits chaos through periodic doubling bifurcation from period 4 (Figure 3(e)) to period 2 (Figure 3(f)) and then to period 1, then stabilizes on main harmonic movement (Figure 3(g)). If the crack progresses further and becomes very large, there develops new resonance region in which the transverse oscillation and swing vibration diverge to infinite quickly. The resonance happens in both sub-critical region and super-critical region. In Figure 4, with time increase, the amplitude of response goes to an unlimited extent quickly, which can be considered divergence in rotor system. The deeper the crack is, the wider the chaos range of Ω is. In Table 1, when the crack is fairly large, there will appear chaos near $\Omega=0{\cdot}7848$. Then with the increase of crack (correspondingly p becomes smaller gradually), the chaotic region of Ω becomes wider. If the crack is extremely large, oscillation of the disc will go infinitely. Figure 5 shows that with the increasing of crack, the response becomes chaos from quasi-periodic intermittence, and then exits chaos also from quasi-period, finally Hopf bifurcation happens and the response becomes periodic-1 movement. When $p=0{\cdot}706$, the response is a stable quasi-periodic movement (Figure 5(a)). Then crack increases ($p=0{\cdot}703$), the quasi-periodic movement losses stability and becomes

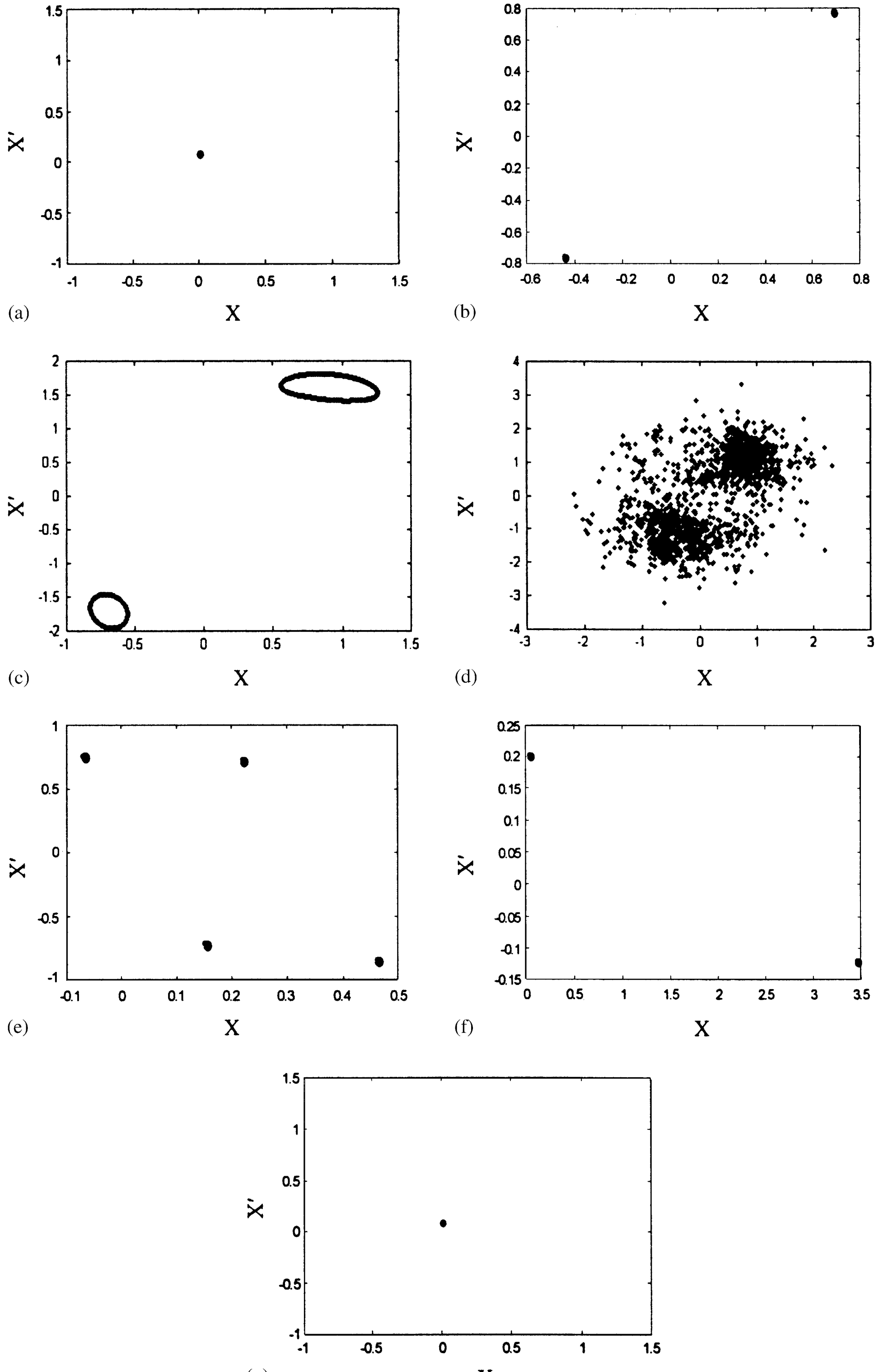

Figure 3. Influence of speed ratio Ω on disc response ($p = 0{\cdot}5$, $D = 0{\cdot}02$): (a) $\Omega = 1{\cdot}3536$ (Poincaré map), (b) $\Omega = 1{\cdot}3630$ (Poincaré map), (c) $\Omega = 1{\cdot}3645$ (Poincaré map), (d) $\Omega = 1{\cdot}3646$ (Poincaré map), (e) $\Omega = 1{\cdot}3649$ (Poincaré map), (f) $\Omega = 1{\cdot}3678$ (Poincaré map) and (g) $\Omega = 1{\cdot}3720$ (Poincaré map).

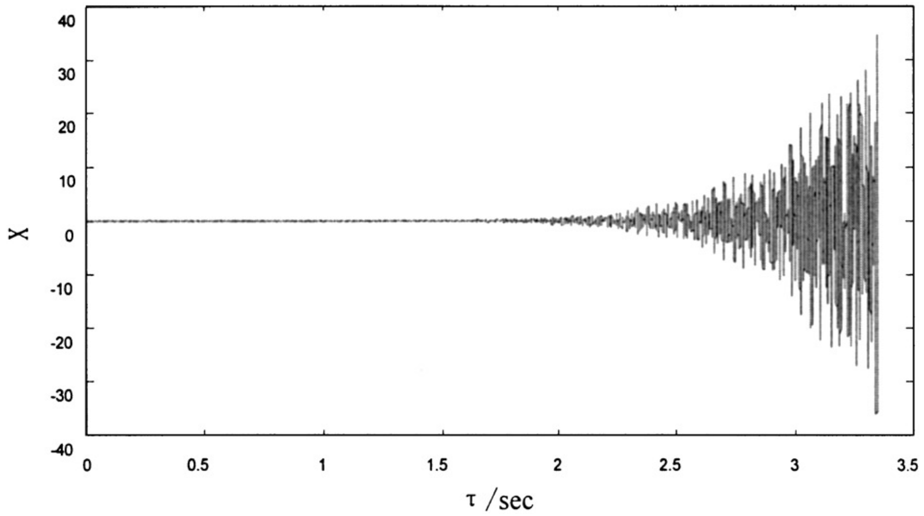

Figure 4. For large crack response amplitude increases quickly to divergence (wave form) ($\Omega = 1{\cdot}7$, $p = 0{\cdot}3$, $D = 0{\cdot}01$).

intermittence chaos (Figure 5(b) and 5(c)). When $p = 0{\cdot}650$, response becomes complete chaos (Figure 5(d)). At $p = 0{\cdot}620$, response exits chaos and returns to quasi-periodic movement (Figure 5(e)), and then response becomes periodic movement through Hopf bifurcation (Figure 5(f)).

3.3. INFLUENCE OF CRACK ANGLE β

The change of crack angle β will not affect the essence of the disc's movement. If response is chaotic, quasi-periodic or periodic at $\beta = 0$, response will also be chaotic, quasi-periodic or periodic at the other crack angle. But the pin–pin value of the synchronous component of the response is variable with angle β. Figure 6 shows the variation of pin-pin value of the synchronous oscillation at sub-critical speed and super-critical speed with angle β. As β changes from 0 to 2π, the pin-pin value is smallest at $\beta = \pi$ and is largest at $\beta = 0$ or 2π. In sub-critical speed, it is obvious that the amplitude decreases sharply at $\beta = \pi$ because there appears $2X$ harmonic component in the response here.

TABLE 1

The chaotic region near Ω=0·7848 with different crack depth (p)

P	Chaotic region of Ω	Length of chaotic region ($\Delta\Omega$)
0·49	0·7886–0·7923	0·0037
0·45	0·7848–0·7933	0·0085
0·41	0·7815–0·7967	0·0152
0·37	0·7744–0·7952	0·0208
0·33	0·772 –0·7948	0·0228
0·30	0·7692–0·7943	0·0251

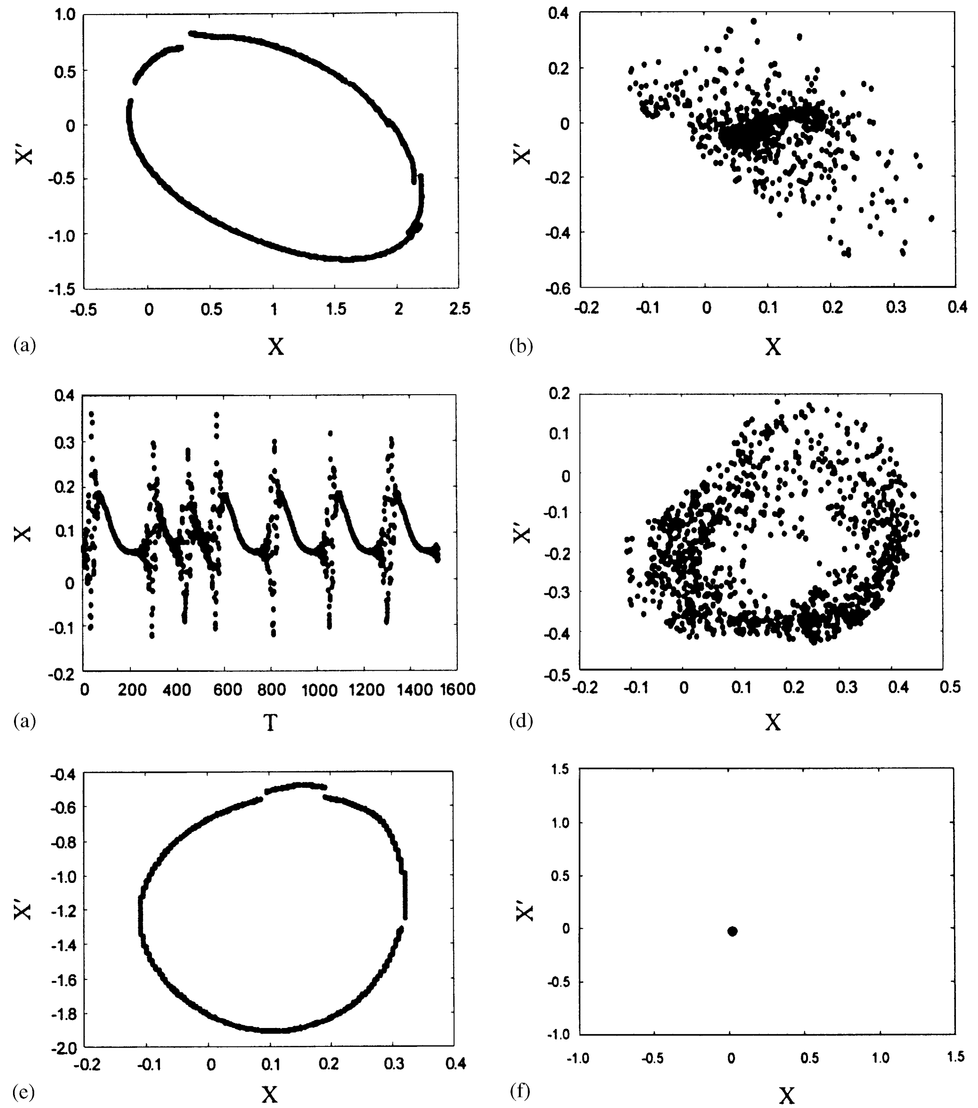

Figure 5. Influence of crack depth on disc response ($\Omega = 1{\cdot}0583$, $D = 0{\cdot}02$): (a) $p = 0{\cdot}706$ (Poincaré map), (b) $p = 0{\cdot}703$ (Poincaré map), (c) $p = 0{\cdot}703$ (diagram of time-phase), (d) $p = 0{\cdot}650$ (Poincaré map), (e) $p = 0{\cdot}620$ (Poincaré map) and (f) $p = 0{\cdot}600$ (Poincaré map).

3.4. INFLUENCE OF UNBALANCE PARAMETER U

For synchronous oscillation, the response amplitude may increase or decrease with the increasing of U depending on the crack angle β and the relative value of unbalance and crack. The influence of crack on synchronous component of the response could be looked as an equivalent unbalance and the combined influence of this equivalent unbalance and the original unbalance will determine the changing of vibration amplitude. For non-synchronous response, when $\beta = 0$, the increase of U will in some cases make the response unstable in sub-critical region and stable in super-critical region; it is just the opposite when $\beta = \pi$. As shown in Figure 7, when $\beta = \pi$, $\Omega = 0{\cdot}7$, the response is chaotic for $U = 0{\cdot}2$,

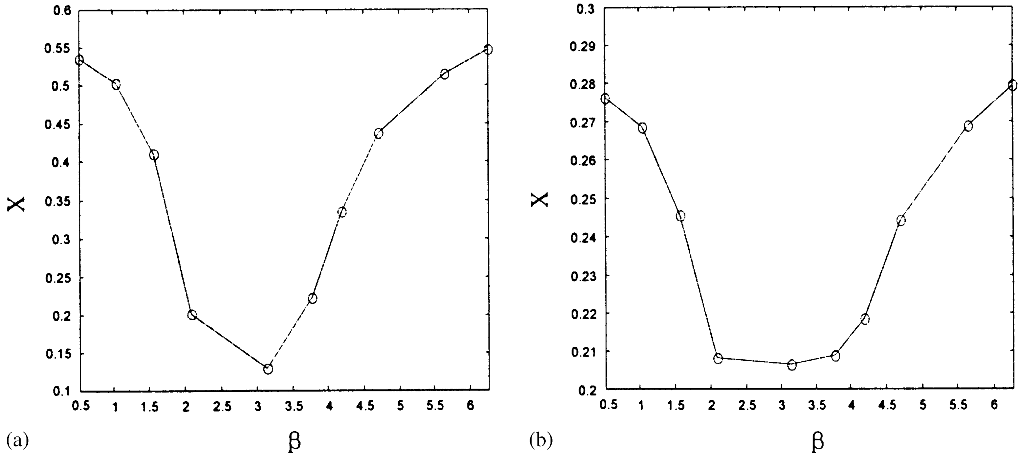

Figure 6. Variation of pin–pin value of response in sub-critical and super-critical region with β ($p=0{\cdot}7$): (a) $\Omega=0{\cdot}71$ and (b) $\Omega=1{\cdot}71$.

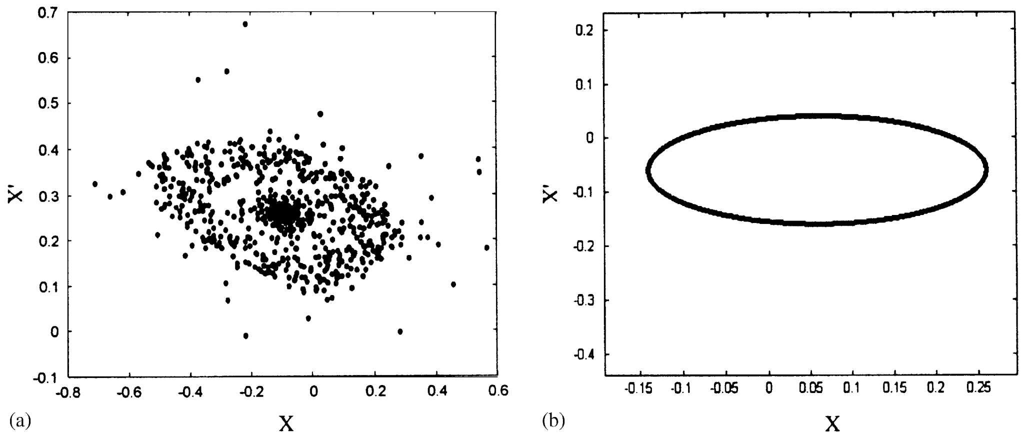

Figure 7. Influence of unbalance parameter U on disc response ($\beta=\pi$, $\Omega=0{\cdot}7$): (a) $U=0{\cdot}2$ (Poincaré map) and (b) $U=1{\cdot}2$ (Poincaré map)

becomes quasi-periodic as U increases to $1{\cdot}2$ and stabilizes on quasi-periodic as U increases further.

3.5. ROUTES TO CHAOS

For cracked rotor, the main route of transverse oscillation and swing vibration to chaos is intermittence. There also exists route of quasi-period to chaos (see Figure 3). Although there exist the routes of doubling periodic bifurcation to chaos, they are scarcely observed; this is because when response begins to bifurcate, the effect of opening and closing of the crack makes the response lose stability and become stable quasi-periodic directly. Intermittence chaos can start from both periodic and quasi-periodic movement.

Figure 8 shows the time phase of the typical phenomenon of intermittence from quasi-period. By observing carefully, it is found that the intermittence chaos results from the

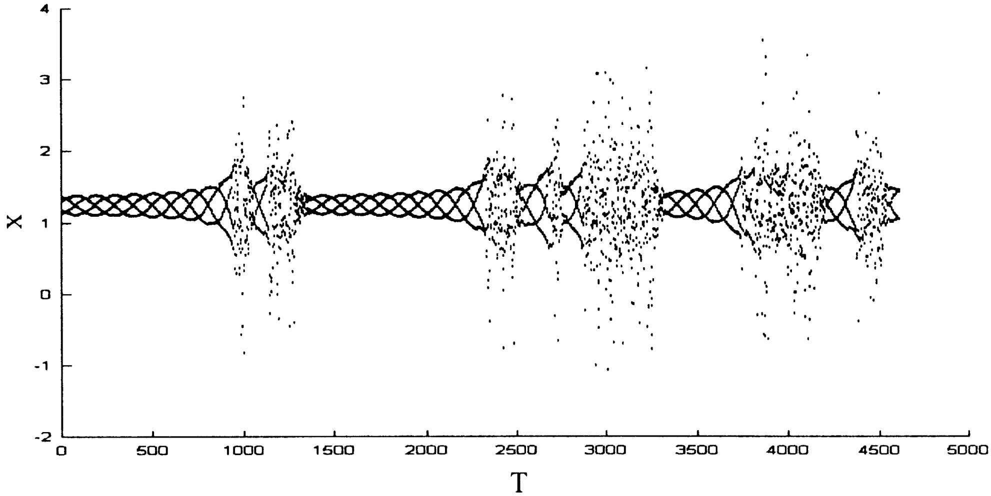

Figure 8. Diagram of time phase of intermittence chaos from quasi-period ($\Omega = 1{\cdot}1675$, $D = 0{\cdot}01$, $p = 0{\cdot}5$).

increase of amplitude of swing vibration. When intermittence chaos begins, the oscillation is stable, and the amplitude of swing vibration keeps increasing continuously till the stable oscillation is broken. Then the amplitude of swing vibration decreases rapidly and the oscillation restores stable movement gradually, the oscillation is broken again after the stable movement for a period of time. This process constructs intermittence chaos. With the change of parameters to worse, the stable oscillation is broken more often and the response becomes chaotic finally. As Figure 9 shows, when $\Omega = 1{\cdot}5961$, the intermittence chaos begins and the periodic-1 movement is broken at a fairly long interval (Figure 9(a)). And then, when $\Omega = 1{\cdot}5989$, the periodic-1 movement is broken more frequently (Figure 9(b)). Finally at $\Omega = 1{\cdot}6055$, the periodic response is broken very frequently and can be regarded as a complete chaotic movement (Figure 9(c)).

4. SUMMARY AND CONCLUSION

Since the cracked rotor is difficult to be analyzed, the numerical simulation is still an effective method at present. From the above simulation results, the following conclusions can be obtained.

(1) For the diagnosis of crack fault, the swing vibration is meaningful. If there is no crack, there is no swing vibration (for Jeffcott rotor). If small crack occurs, swing vibration will happen and the swing vibration includes many harmonic components. In other words, the swing vibration is sensitive to the occurrence of crack. This is helpful for crack diagnosis.
(2) For cracked Jeffcott rotor, the main route to chaos is intermittence. There also exists quasi-period to chaos. The doubling periodic bifurcation to chaos is not easy to be observed. The intermittence chaos starts from either period or quasi-period. The appearance of intermittence chaos results from the fact that the amplitude of swing vibration increases and the stable oscillation is frustrated.
(3) When the crack becomes deep, there will be chaotic response. If the crack is very deep, there appear some new resonance regions in which the response will go to infinite. These regions exist in both sub-critical and super-critical regions.

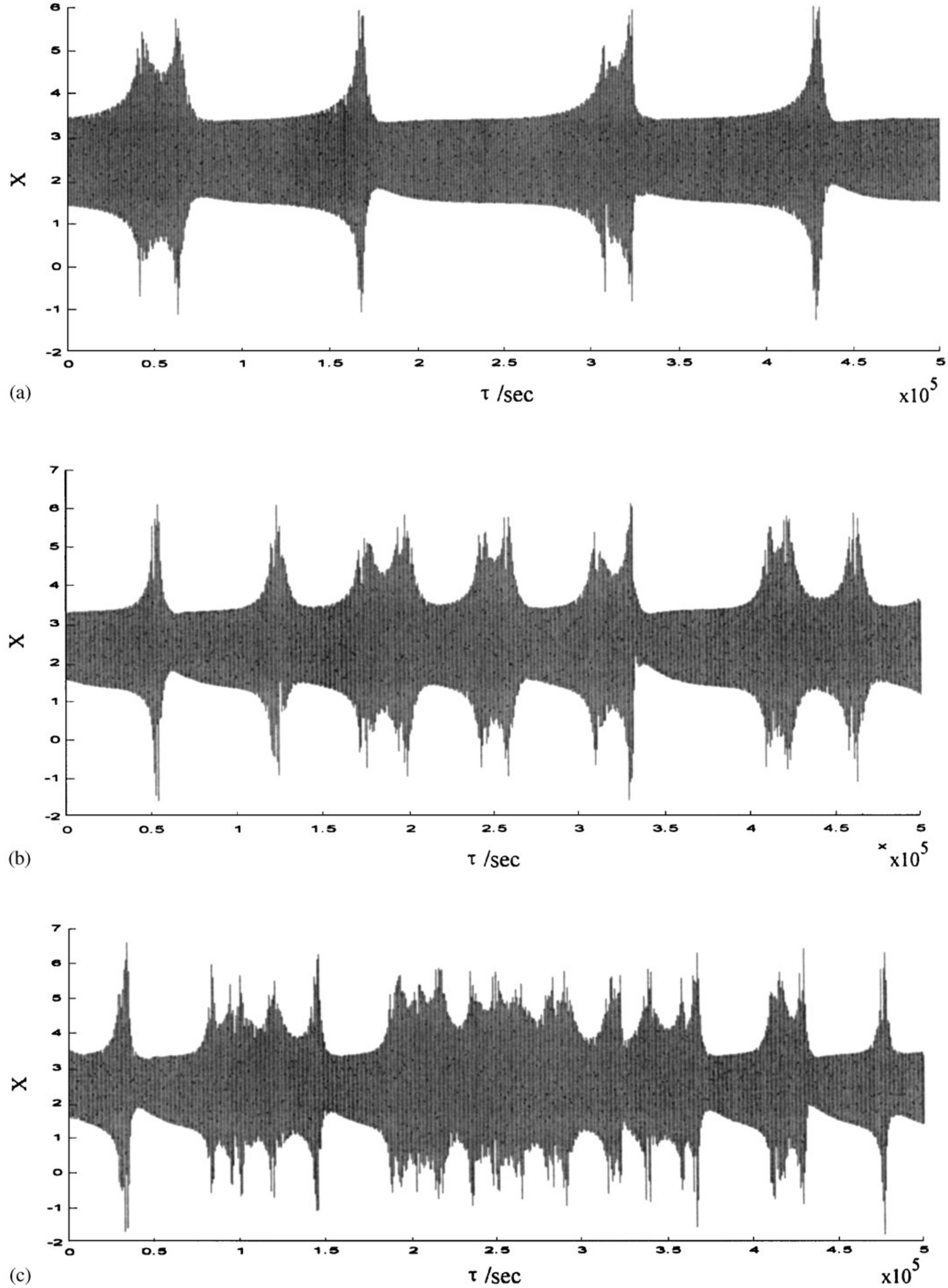

Figure 9. Development of intermittence chaos from period-1 with change of speed ratio Ω (wave form) ($p=0{\cdot}7$, $D=0{\cdot}04$): (a) $\Omega=1{\cdot}5961$ (wave form), (b) $\Omega=1{\cdot}5989$ (wave form) and (c) $\Omega=1{\cdot}6005$ (wave form).

(4) Unbalance parameter U is effective in suppressing chaos. If U is fairly large, the chaos will be fixed to stable movement. Crack angle β can affect the synchronous response, but it cannot affect the essence of non-synchronous and synchronous response.

ACKNOWLEDGMENTS

The supports from the National Natural Science Foundation of China (No. 19502010) and the China 10-5 State Key Project (No. 2001BA204B05-KHKZ0009) are gratefully acknowledged.

REFERENCES

1. A. R. JACK and A. N. PATTERSON 1976 *1st Mechanical Engineering Conference (The Influence of the Environment on Fatigue)*. Cracking in 500 MW LP rotor shafts.
2. P. C. MULLER, J. BAJKOWSKI and D. SOFFKER, 1994 *Nonlinear Dynamics*, **5**. Chaotic motions and fault detection in a cracked rotor.
3. A. S. SEKHAR 2000 *Shock and Vibration Digest*, 3**2**. Vibration characteristics of a cracked rotor with two open cracks.
4. G. T. ZHENG and A. Y.T. LEUNG 1998 *Journal of the Chinese Society of Mechanical Engineers, Transactions of the Chinese Institute of Engineers, Series C* **19**, 125–133. On the stability of cracked rotor systems.
5. A. W. LEES and M. I. FRISWELL 1999 *Key Engineering Materials* **167**, 246–255. Crack detection in asymmetric rotors.
6. G. MENG and R. GASCH 2000 *Transaction of the American Society of Mechanical Engineers, Journal of Vibration and Acoustics* **122**, 116–125. Stability and stability degree of a cracked flexible rotor supported on journal bearings.
7. J. B. ZHENG and G. MENG 1998 *International Journal of Bifurcation and Chaos* **8**, 597–607. Bifurcation and chaos response of a nonlinear cracked rotor.

APPENDIX A: NOMENCLATURE

m	mass of disc
C_d	external damping
δ	static deflection (= mg/k)
J_d	moment of inertia of disc with respect to a diameter
k	stiffness of uncracked shaft
k_θ	angular stiffness of uncracked rotor
e	the unbalance eccentricity
k_ξ, k_η	stiffness of crack shaft in ξ and η direction
$k_{\theta\xi}$, $k_{\theta\eta}$	angular stiffness of crack shaft in ξ and η direction
Δk	largest stiffness change in ξ direction
Δk_θ	largest angular stiffness change in ξ direction
ΔK_d	stiffness change ratio ($=\Delta k/k$)
ΔK_θ	angular stiffness change ratio ($=\Delta k_\theta/k_\theta$)
I_z	moment of inertia of shaft section at crack position
D	external damping ratio ($=c_d/2m\omega_c$)
ω	rotating speed
x, y	deflection of disc
θ_x, θ_y	angular deflection of disc
p	ratio of I_z and I_0 ($= I_z/I_0$)
J_p	polar moment of inertia of disc

X, Y	non-dimensional deflection ($=x/\delta$, y/δ)
U	unbalance parameter ($=e/\delta$)
β	angle between crack and unbalance
ϕ_e	initial unbalance angle
ξ, η	body fixed rotating co-ordinate, ξ is in the direction of crack
ω_c	rigid critical speed ($=$ (k/m)$^{1/2}$)
ω_{ac}	rigid angular critical speed ($=$ $(k_\theta/J_d)^{1/2}$)
Ω	speed ratio ($= \omega/\omega_c$)
Ω_1	speed ratio ($= \omega/\omega_{ac}$)
I_0	moment of inertia of uncracked rotor
τ	($=\omega t$)
ω_r	response frequency